Observed Climate–Snowpack Relationships in California and their Implications for the Future

SARAH KAPNICK AND ALEX HALL

University of California, Los Angeles, Los Angeles, California

(Manuscript received 27 October 2008, in final form 11 December 2009)

ABSTRACT

A study of the California Sierra Nevada snowpack has been conducted using snow station observations and reanalysis surface temperature data. Monthly snow water equivalent (SWE) measurements were combined from two datasets to provide sufficient data from 1930 to 2008. The monthly snapshots are used to calculate peak snow mass timing for each snow season. Since 1930, there has been an overall trend toward earlier snow mass peak timing by 0.6 days per decade. The trend toward earlier timing also occurs at nearly all individual stations. Even stations showing an increase in 1 April SWE exhibit the trend toward earlier timing, indicating that enhanced melting is occurring at nearly all stations. Analysis of individual years and stations reveals that warm daily maximum temperatures averaged over March and April are associated with earlier snow mass peak timing for all spatial and temporal scales included in the dataset. The influence is particularly pronounced for low accumulation years indicating the potential importance of albedo feedback for the melting of shallow snow. The robustness of the early spring temperature influence on peak timing suggests the trend toward earlier peak timing is attributable to the simultaneous warming trend (0.1°C decade^{-1} since 1930, with an acceleration in warming in later time periods). Given future scenarios of warming in California, one can expect acceleration in the trend toward earlier peak timing; this will reduce the warm season storage capacity of the California snowpack.

1. Introduction

The California water supply is determined by cold season precipitation (rain in low elevations and snow in high elevations) and the capacity of natural and manmade reservoirs. Most manmade reservoirs were built in the early twentieth century for two purposes: 1) the storage and disbursement of cold season rains and 2) the storage and disbursement of runoff from spring snowmelt. Reservoirs were designed to store only a fraction of the state's total yearly precipitation, under the assumption that a sufficient delay between winter rains and spring snowmelt runoff would always exist, with snowmelt occurring at roughly the same time every year. The annual mountain snowpack thus provides natural storage for the water supply until the onset of snowmelt. Changes in the amount of precipitation, percentage of precipitation falling as rain instead of snow, and onset of snowmelt can therefore affect the state's water supply. During anomalously high rain or snowmelt events, reservoirs must not only store water, but also discharge excess water to avoid flooding. Water must sometimes even be discharged in anticipation of large events to reduce flood risk. The dual functions of storage and flood management require reservoir managers to carefully balance factors such as precipitation, snowmelt timing, reservoir storage capacity, and demand. Even if future climatological precipitation remains unchanged, shifts in snowmelt timing can affect California's water supply during the warm season because of reservoir storage capacity constraints. To understand changes in snowmelt water supply as a result of climate change, it is therefore important to understand changes in the timing of snowmelt in addition to total spring snowpack amounts.

Snowpack measurements are essential for predicting timing and amount of warm season snowmelt runoff. For this reason, a network of stations in the western United States dating back to the 1930s tracks water content of snow (also known as snow water equivalent; SWE). Measurements are taken manually around the first of the month at each station according to a prescribed monthly

Corresponding author address: Sarah Kapnick, University of California, Los Angeles, P.O. Box 951565, Los Angeles, CA 90095-1565.
E-mail: skapnick@atmos.ucla.edu

DOI: 10.1175/2010JCLI2903.1

© 2010 American Meteorological Society

schedule. Because of the desire to track peak SWE—thought to occur in early April—many more records are available on or around 1 April (Serreze et al. 1999). Previous snowpack studies have focused on this well-sampled 1 April SWE dataset (Barnett et al. 2008; Mote 2006; Mote et al. 2005; Cayan 1996) to assess the climatology and variability of snowpack in the western United States. These studies are important for understanding total meltwater available during the warm months, but do not directly address the timing of the transition from accumulation to melt from snow observations.

Ideally, high-temporal resolution data would be available to study the evolution of the snowpack over the course of the season, particularly the exact date and amount of maximum SWE and subsequent melt rates. Stations have been built in California since the 1970s to measure daily SWE automatically, but do not begin early enough for long-term variability analysis. Previous observational studies have instead utilized streamflow data, presumably snowmelt-dominated, as a proxy for snowmelt timing. They show there has been a trend in streamflow discharge toward earlier in the spring using a variety of streamflow metrics (Regonda et al. 2005; Stewart et al. 2005; Cayan et al. 2001). Daily SWE data from 1992 to 2002 has also been combined with long-term historic streamflow data to study the onset of spring in the Sierra Nevada (Lundquist et al. 2004); however, because of the shortness of the SWE time series, streamflow measurements must still be relied upon to measure long-term variability in snowmelt. Unfortunately, this indirect variable is not a perfect measure of snowmelt, as it can be influenced by other factors such as precipitation, temperature, lithology, soil composition, vegetation (Aguado et al. 1992), and presnowmelt soil moisture.

Modeling studies to produce SWE, temperature, and precipitation values have also been conducted to assess changes in the snowpack of the Western United States. Hamlet et al. (2005) created a snowpack simulation from 1915 to 2003 using the variable infiltration capacity hydrologic model as a surrogate for historical SWE observations and found that downward trends in 1 April SWE and trends toward earlier peak snow accumulation were due to warming over the period. Pierce et al. (2008) produced simulations for 1600 years using two global circulation models, yielding evidence that SWE as a percentage of precipitation has had a negative trend because of anthropogenic forcing that will continue in the future. These modeling studies show that the Sierra snowpack has been declining and project a continuance of a negative trend in SWE in the future.

To study changes in the California snowpack directly and provide a purely empirical sensitivity for future projections, the present study focuses on observations of monthly SWE. A dataset has been compiled from two different sources to provide sufficient stations with SWE measurements from mid-January through mid-May over a long enough time period to do robust trend and sensitivity analysis. The monthly data is used to infer peak snow mass timing from February to May. Over this record stretching roughly from 1930 to the present, the peak timing exhibits a trend toward earlier in the season. Much of this trend can be explained by the sensitivity of snow mass peak timing to early spring temperature. Given future warming scenarios in the California Sierra Nevada, we conclude the trend in earlier peak timing will continue.

2. Data

A snow station dataset was compiled from two existing datasets for the state of California: the National Resources Conservation Service (NRCS) and Water and Climate Center (www.wcc.nrcs.usda.gov/snowcourse/) and the California Department of Water Resources (http://cdec.water.ca.gov/misc/SnowCourses.html). A total of 154 stations across California with recorded SWE data from mid-January to mid-May with at least 30 years of data from 1930 to 2008 are used (see Fig. 1). These stations range in their years of available data. We show that these temporal gaps have a negligible impact on our analysis in the appendix. It has been noted that the exact timing of historical monthly snow course measurements can vary, with some measurements being taken within a few days of the first-of-the-month measurement date (Cayan 1996). In these measurements, there may also be a systematic shift in the actual date of measurement toward later (Mote et al. 2005). To circumvent these issues we only selected stations with exact measurement dates corresponding to raw SWE data for our analysis. The correlations shown in this paper are noticeably reduced when SWE values are assumed to be first-of-the-month values; such employment of SWE measurements may therefore lead to a nonnegligible source of random error in the other studies. Subsequent sections will describe criteria used to produce subsets of data for analysis.

Temperature data are also used to diagnose snow accumulation and melt processes. Maximum and minimum daily temperature data from 1930 to 2003 were obtained from the Surface Water Modeling group at the University of Washington from their Web site (www.hydro.washington.edu/Lettenmaier/Data/gridded/) the development of which is described by Hamlet and Lettenmaier (2005). This dataset was chosen for its long temporal coverage (1915–2003) and high spatial resolution ($^1/_8°$) relative to other pre-satellite-era temperature products.

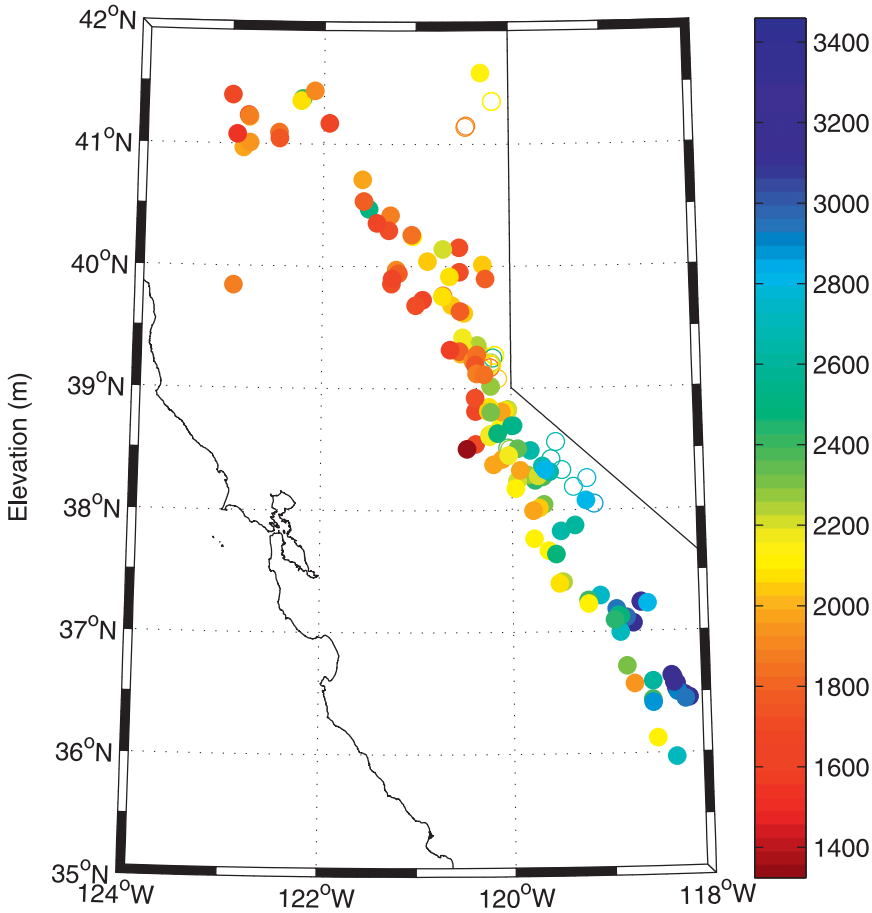

FIG. 1. Location of 154 snow stations with usable data in California. Open circles denote NRCS Water and Climate Center stations and closed circles denote California Department of Water Resources stations. Stations are colored by elevation in meters.

This product has also been used in previous snowpack studies (Mote et al. 2005; Hamlet et al. 2005).

3. Methods and results

a. Calculation of snow mass peak

To assess interannual variations in California snowpack evolution, a metric was developed quantifying systematic changes in snow accumulation and melt timing. In particular, we focused on the timing of peak snow mass. We created a measure of this quantity relying on SWE measurements taken around the first-of-the-month from February to May. We used these monthly snapshots rather than daily SWE data because the daily data are only robustly available from 1980 to the present, too short a time series to calculate long-term trends in maximum SWE timing.

The peak snow mass timing is defined for any given year as the temporal centroid date, also known as the center of mass, of SWE values (SWE centroid date; SCD) from approximately 1 February to 1 May for stations with complete data over this four-month time period. The SCD is given by the equation:

$$\mathrm{SCD} = \frac{\sum t_i \mathrm{SWE}_i}{\sum \mathrm{SWE}_i}. \tag{1}$$

Each individual measurement during the season is distinguished by i. The SWE measurements are given by SWE_i in centimeters. The value t_i is the exact date of the measurement in Julian days and falls within two weeks of the first of the month for February, March, April, and May. The SCD metric is similar to that used in previous studies of streamflow peak timing (Stewart et al. 2004, 2005). Figure 2a provides a visualization of this calculation for a location and a year when daily data are also available. As is clear from the figure, SCD captures the gross timing of snow processes. For the peak to shift earlier

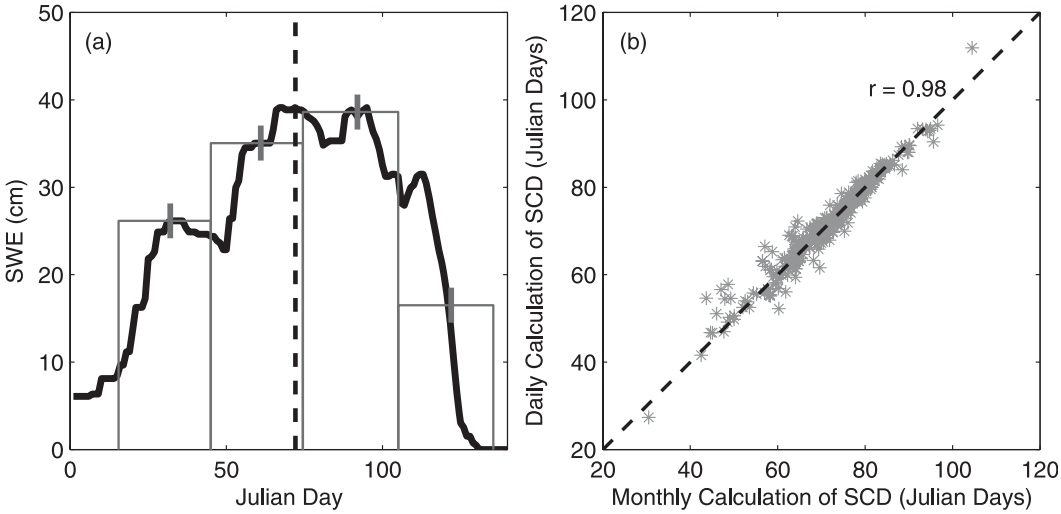

FIG. 2. SCD monthly calculation example for (a) one station in 1996 and (b) a comparison of the monthly vs daily calculations of SCD for 13 stations. In (a), the solid black line denotes daily 1996 SWE values at the SNOTEL Adin Mountain station from 1 January to 31 May. The gray bars help illustrate how four measurements of SWE values are used to calculate the SCD over the time period shown. The gray hatch on each bar denotes the first of February, March, April, and May. The black dashed line at Julian day 72 denotes the SCD found by using the monthly SCD values. In (b), 13 stations with daily data were used to calculate SCD using the daily and monthly methods. The stations were chosen by their proximity to stations used in the long trend analysis shown in Fig. 3. The monthly approximation of SCD is well correlated with the daily calculation of SCD ($r = 0.98$, $p < 0.01$). There are 336 data points for 13 stations from 1970 to 2008.

(later), the percentage of snow accumulation later in the season must decrease (increase), or there must be an increase (decrease) in the percentage of snow melting later in the season. Thus it corresponds roughly with the peak in snow mass.

The SCD metric provides a more accurate representation of the timing of snow accumulation and melt than the date of absolute maximum SWE value given in the four approximate first-of-the-month point measurements. It allows for the snow mass peak timing to shift on the order of days instead of being constrained to shifts in monthly increments. Long-term variability in snow mass peak timing can be studied on submonthly time scales despite the lack of daily data. As we show below, the changes in peak snow mass timing in the California Sierra Nevada are on the order of days, confirming the need for a metric with this property.

For stations where daily data are available within close proximity to long-term monthly stations, SCD was calculated on a daily and monthly basis to assess the accuracy of using historical monthly SWE values. Daily SWE values from 15 January to 15 May from 13 stations were used to calculate a daily SCD, while first-of-the-month measurements taken from the daily stations were used to calculate a monthly SCD. These stations were chosen to correspond to those used in subsequent long-term monthly trend analysis. For each station, years missing 10 or more days from January to May were excluded; this criterion was similarly employed by Knowles et al. (2006) and developed by Huntington et al. (2004). The SCD values calculated from monthly and daily data was found to be extremely highly correlated ($r = 0.98$, $p < 0.01$), giving confidence that the temporal resolution of monthly snapshots is high enough to provide accurate information about snowpack timing.

b. *Trends in peak snow mass timing*

Examination of SCD from 1930 to 2008 yields evidence that it is trending earlier. When stations with data for at least 75% of these years are included, SCD is found to occur earlier at a rate of 0.6 days per decade (Fig. 3; this is similar to figures showing trends in earlier spring timing in Cayan et al. (2001)). This trendline has a slope significantly different than zero (using the Student's t test, $p < 0.01$). When stations with fewer yearly SCD values are also included, or when the starting year of the trendline is set later to include more stations, statistically significant nonzero trendlines of earlier peak timing are still found (Table 1). In most cases, the trend toward earlier peak timing is enhanced (i.e., the trend becomes more negative). There is a similar enhancement in the averaged March and April maximum daily temperature warming trend from 1930 to 1970 as successively

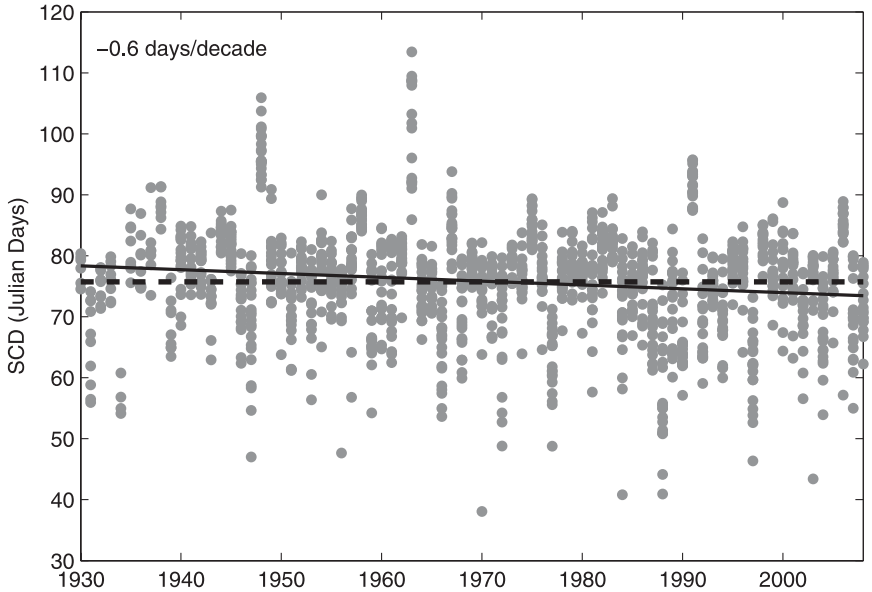

FIG. 3. SCD for 22 stations with annual data available for at least 75% of the record from 1930 to 2008. There are 1482 data points for the time period. The dashed line denotes the mean SCD (Julian day 76) and the solid line denotes the linear trendline for the time series.

later periods of the time series are isolated (Table 1, last row). We discuss the potential causal link between the warming and SCD trends in the discussion.

Almost all individual station SCD trends are also negative (Fig. 4), suggesting a consistent signal from catchment to catchment. In addition, Fig. 4 compares station trends in SCD to trends in the highly studied 1 April SWE record. Note that measurements are taken within two weeks of 1 April for the 1 April SWE record. Mote et al. (2005) noted that the fluctuation in measurement date may affect 1 April SWE trends, but concluded that climatic factors likely have a dominant effect on the trend. The majority of stations exhibit a negative trend in both SCD and 1 April SWE. A negative SCD trend is associated with snow melting earlier, which also results in trends toward lower SWE. Some of the change in SCD may also be driven by a shift toward more rain and less snowfall as described by Knowles et al. (2006); our analysis shows that only the lowest elevation stations have exhibited statistically significant trends in both metrics.

Figure 4 resolves the apparent inconsistency between increasing 1 April SWE at some locations and a warming climate. All the points with positive trends in 1 April SWE have negative trends in SCD. These points all have positive trends in SWE from February to May (not shown). Enhanced melting at these locations must therefore be compensating for the increased accumulation to create the negative trend in SCD. The link between 1 April SWE values and melt during previous months has been observed in some daily Snowpack Telemetry (SNOTEL) stations in the California Sierra Nevada; 1 April SWE was shown to be highly anticorrelated with daily melt events from the previous months, implying changes in 1 April SWE have been due at least in part to melt events (Mote et al. 2005).

TABLE 1. Trend in peak timing (days decade^{-1}) for collective stations and temperature (°C decade^{-1}) found in the grid cells covering the snow stations from start date (denoted in columns) to 2008. Trend in peak timing is given for three different cases: all stations with available SCD data, stations with data for only 50% of available years, and stations with data for only 75% of available years. The SCD trend corresponding to Fig. 3 is given by the bolded cell. Trend in average monthly maximum daily temperature at elevations above 1700 m (elevation minimum for snow stations used in the bulk of this analysis) is given from start date to 2003 (due to the limitation of the available temperature dataset) for the months of January, February, March, and April with the last row providing the averaged March and April temperature trend.

Case	1930	1940	1950	1960	1970
All Stations	−0.7	−0.8	−0.7	−0.7	−0.4
50% of years	−1.0	−1.1	−0.7	−0.7	−0.7
75% of years	**−0.6**	−0.9	−0.8	−1.0	−0.5
January temperature	0.3	0.3	0.5	0.5	0.7
February temperature	0.2	0.2	0.1	0.0	−0.1
March temperature	0.2	0.3	0.4	0.5	0.7
April temperature	0.0	0.1	0.1	0.3	0.5
May temperature	0.1	0.2	0.3	0.3	0.2
Averaged March and April temperature	0.1	0.2	0.3	0.4	0.6

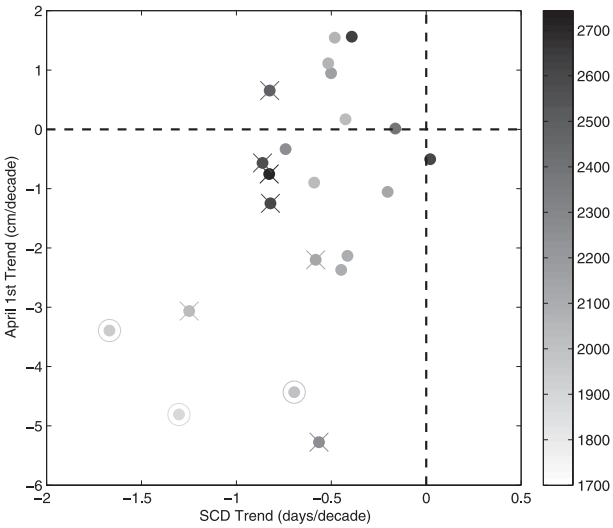

FIG. 4. Trend in SCD vs trend in 1 April SWE for 22 stations with at least 75% of years available from 1930 to 2008. Stations are the same ones used for Fig. 3. Dashed lines denote trends of zero. Stations are colored by elevation in meters. Circled stations have statistically significant trends (at $p < 0.05$) in 1 April SWE and SCD. Stations with a cross (x) have statistically significant trends (at $p < 0.05$) in 1 April SWE or SCD.

c. *Distribution of peak snow mass timing versus 1 April SWE*

Variability in 1 April SWE is evaluated against variability in the SCD metric to explore relationships between SCD and the SWE variable used to predict water supply. Figure 5 shows a scatterplot of 1 April SWE versus SCD values. Each point represents a snow station during one snow season. Snow stations with a minimum of 75% of SCD values over the period from 1950 to 2003 were used for this analysis. This time period was selected to coincide with the available temperature record and increase the number of snow stations available for temperature sensitivity studies in section 3d. (A nearly identical distribution is found if the start date is changed to 1930.) For the given subset of snow stations, SCD occurs over a wide range, with the average SCD occurring on Julian day 73 (mid March). The average 1 April SWE value is 74 cm.

The striking bell-shaped distribution of the 1 April SWE versus SCD scatterplot arises because of differing behavior of SCD for large and small seasonal snow accumulation. When 1 April SWE is large (roughly ≥100 cm), the SCD tends to occur in a narrow band between Julian day 70 and 90, with most points (96%) above the mean of 73. This corresponds to a time period mainly falling between the middle of the second and third bar of Fig. 2, or the calendar month of March. There are three main reasons for this behavior: 1) To attain such high 1 April SWE values, relatively consistent storm activity and steady accumulation is necessary from February to March. 2) The large accumulation then increases the effective thermal inertia of the snowpack, delaying the onset of melting. 3) This large accumulation then only melts once the seasonal warming becomes great enough to initiate the melting process. These three processes make for a late SCD, with little variation from season to season.

When 1 April SWE is small (less than roughly 100 cm) however, the SCD falls over a large range between Julian day 21 and 114. This range is more than 4 times that of the high seasonal accumulation and covers the middle of the first bar to the middle of the fourth bar in Fig. 2, or from the last day in January to the end of April. The significantly greater range in SCD values is due to two factors: 1) Low accumulation is the result of a relatively small number of storms with highly variable timing. 2) Melting in shallow snow is more sensitive to temperatures above freezing because of the smaller thermal inertia of shallow snow and its greater susceptibility to albedo feedback. This results in earlier (later) snowmelt when temperatures are warm (cold).

To explore the sensitivity of SCD to temperature further, the colorbar given in Fig. 5 distinguishes the distribution of SCD values by local averaged March and April (MA) maximum daily temperature. The local average maximum daily temperature for each station is calculated by taking the local gridcell maximum daily temperature, averaging it over two months, and adjusting it for the elevation of each station assuming a constant lapse rate of 6.5°C km^{-1}. When the distribution of SCD versus 1 April SWE is distinguished by temperature, SCD has very little systematic association with either January or February temperatures, but is closely linked to early spring temperature (colorbar in Fig. 5). The correlations of observed SCD and temperatures for different months are shown in the first row of Table 2, and clearly quantify the influence of late accumulation season temperature on SCD. Lower MA temperatures appear to shift SCD into the later half of the season. The most likely reason for this connection is that snowmelt during March and April is reduced (increased) by anomalously cold (warm) March and April temperatures, thus moving SCD to the later (earlier) portion of the season. The sensitivity to MA temperature is particularly pronounced for years when 1 April SWE is low ($r = -0.61$, $p < 0.01$ when 1 April SWE is less than 100 cm versus $r = -0.47$, $p < 0.01$ when it is above this threshold), providing direct evidence of the greater susceptibility of shallow snow to fluctuations in temperature and potentially albedo feedback.

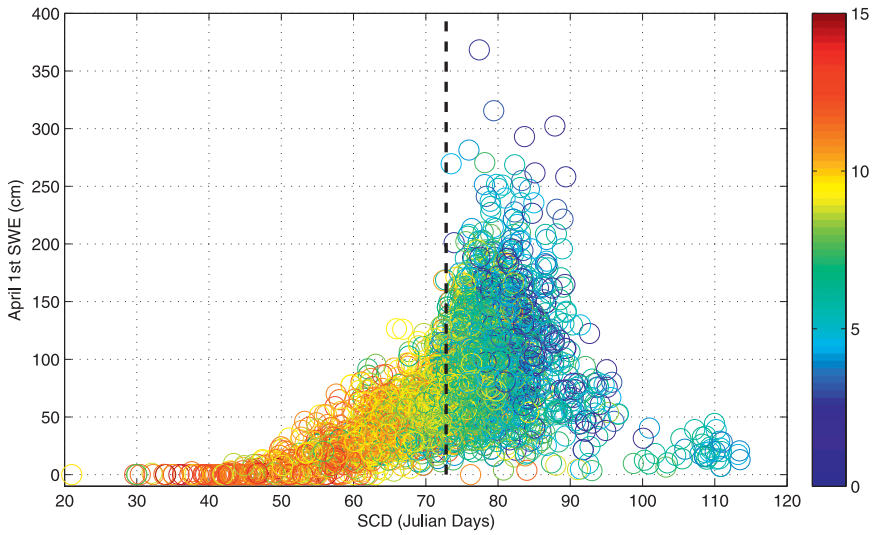

FIG. 5. Scatterplot of SCD vs 1 April SWE value for 70 stations with at least 75% of years available from 1950 to 2003; colored by the local averaged March and April daily maximum temperature. Temperature data are from the Hamlet and Lettenmaier (2005) dataset (available from 1915 to 2003) and have been adjusted for station elevation assuming a constant lapse rate of 6.5°C km^{-1}. If the graph is confined to stations with at least 75% of years available from 1930 to 2003, a similar distribution is found. The average SCD for the dataset is Julian day 73, and is given by the dashed black line.

d. Relationships between peak snow mass timing and temperature

Figure 5 provides visual evidence that air temperature, the primary thermodynamic control of melt, is potentially a major variable affecting SCD. Figure 6a provides a statistical measure of the link between the MA maximum daily temperature and SCD for the direct observations of these variables. Temperature is found to shift SCD earlier in the season by 2.5 days per degree and is significantly anticorrelated ($r = -0.62$, $p < 0.01$) with SCD. As noted in section 3b, the trend toward earlier SCD coincides with a trend toward warmer MA temperature. The anticorrelation between SCD and temperature seen in Fig. 6a could result from these two trends. However, when the SCD and temperature time series are detrended, the anticorrelation remains ($r = -0.47$, $p < 0.01$). This suggests the link between MA temperatures and SCD is robust for temporal variability as well as trends in SCD, a point we return to in the discussion.

Figures 6b,c reveal the SCD–temperature relationship when controlled for spatial and temporal variability. In Fig. 6b, the temporal SCD and maximum daily temperature anomalies (defined as the observation value minus the mean value at each station) are compared. Here we eliminate any systematic relationship between SCD and temperature in Fig. 6a arising from the fact that the stations are at different locations and therefore have different climatological temperatures. Conversely, in Fig. 6c, temporal variability is eliminated by comparing station mean SCD values against station mean maximum daily temperatures. Thus, each point on the graph is an individual station. A negative relationship between SCD and temperature remains when spatial and temporal variability are each isolated in turn. Moreover, Table 2 shows that MA temperatures have the greatest overall relationship with SCD from January to May for direct observations, anomalies, and mean station values. This analysis was also conducted using averaged daily minimum temperatures; negative correlations

TABLE 2. Correlation of temperature vs SCD for 70 stations from 1950 to 2003 for January–May and for direct observations, anomalies, and mean values of these variables. This table provides a sensitivity analysis of the correlations found in Fig. 6 (the last column, bolded) for different months.

Sensitivity	January	February	March	April	May	**Averaged March and April**
Direct observation	−0.21	−0.21	−0.56	−0.52	−0.28	**−0.62**
Anomaly	0.04	0.02	−0.52	−0.49	−0.10	**−0.65**
Station mean	−0.55	−0.60	−0.65	−0.60	−0.60	**−0.63**

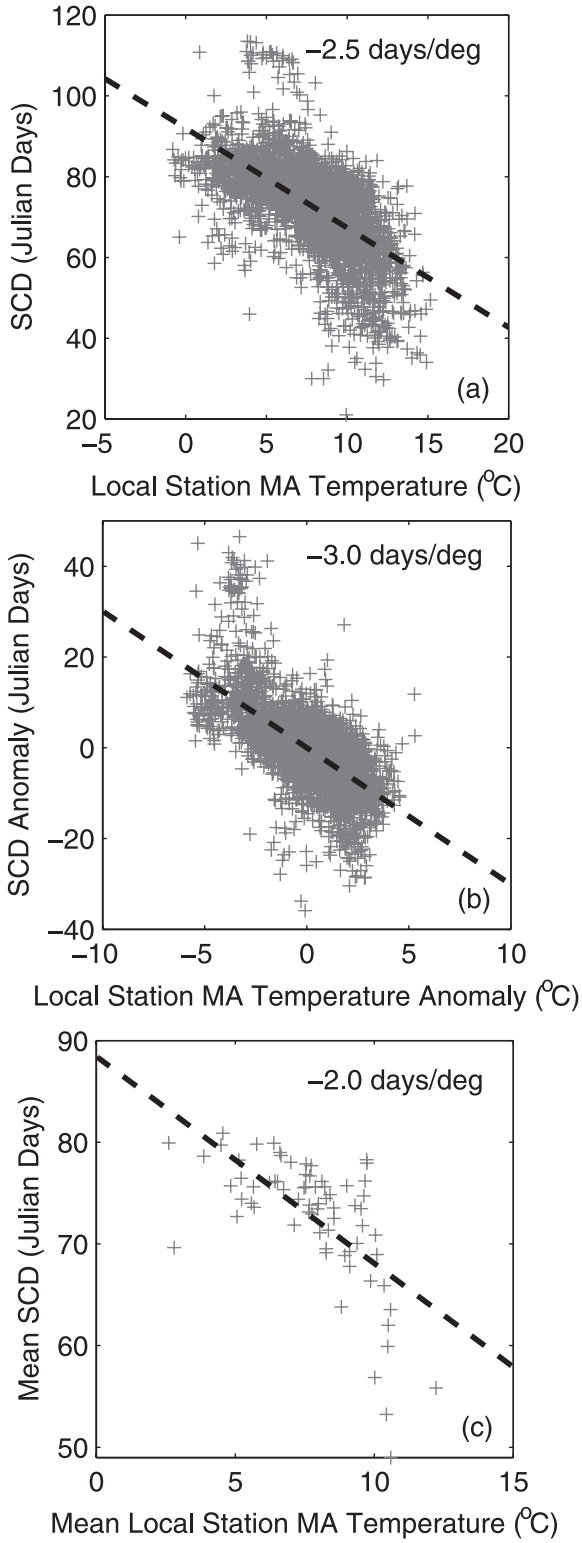

FIG. 6. Scatterplot of averaged March and April daily maximum temperature vs SCD for 70 stations from 1950 to 2003 for: (a) observations of SCD and local temperature, (b) anomalies, and (c) mean values. The dashed black line denotes the linear trendline on each graph. The two variables are strongly anticorrelated for all plots: (a) $r = -0.62$, (b) $r = -0.65$, and (c) $r = -0.63$, with $p < 0.01$ for all graphs. If the correlation is calculated for the detrended direct observations and detrended anomalies, the anticorrelations are slightly lower ($r = -0.47$ in each case), but still material.

between SCD and temperature remained, but were lower than shown in Fig. 6 and Table 2. This is likely due to maximum temperature being more closely associated with snowmelt given that average minimum temperatures are predominantly below freezing. This analysis provides evidence of the predictive value of MA maximum temperature for both spatial and temporal variability in SCD.

4. Summary

In this study, a metric is developed to calculate peak snow mass timing in the California Sierra Nevada using monthly SWE data from 1930 to 2008. Robust statistical analysis is conducted to assess the variability in the timing of peak snow mass. From 1930 to present, the peak timing of the entire dataset exhibits a trend toward earlier in the season of 0.6 days decade^{-1}. On an individual station basis, most stations show earlier SCD and reduced 1 April SWE, and the only stations with statistically significant trends in both SCD and 1 April SWE exhibit negative trends in both variables. The trends in SCD complicate interpretations of 1 April SWE as a metric of Sierra Nevada snowpack trends as nearly all stations exhibit negative trends in SCD indicating that enhanced melting is occurring even when 1 April SWE may be increasing. The influence of MA temperature on SCD is almost certainly due to the effect of early spring temperature on snowmelt. This relationship is particularly pronounced for low accumulation years, indicating the lower thermal inertia of shallow snow and potential enhancement of snowmelt due to albedo feedback as bare ground and vegetation is exposed. The robustness in the sensitivity of SCD to MA temperature for all spatial and temporal scales inherent in the dataset indicates the SCD trend can be attributed to the MA warming trend.

The trend in snow mass peak timing found in this study is less than those of snowmelt-dominated streamflow found in some previous studies (Regonda et al. 2005; Stewart et al. 2005; Cayan et al. 2001), which provide changes in the date of peak runoff on the order of a few days per decade. The differences in the trends in these two metrics may be accounted for by the fact that a shift in the timing of streamflow runoff is not necessarily accompanied by an equal shift in peak snow mass. In fact,

if the shift in SCD is due to earlier snowmelt, the snowmelt acceleration would probably have to be much more rapid than the SCD shift. This is because of the steadiness of the weights of the accumulation months (i.e., measurements around 1 February and 1 March) in the SCD calculation. The involvement of four months of data in the SCD calculation introduces more ''inertia'' into this quantity than snowmelt runoff.

5. Discussion

Taken together, this study and previous studies paint a picture of a California Sierra Nevada snowpack responding rapidly to the changing climate of the past few decades. These trends are likely to continue and may be accelerating. Extrapolating the current trend in MA temperatures, peak snow mass timing should continue to occur earlier. Projections of temperature in California in the coming decades show that the trend in annual temperature may accelerate, with surface temperatures increasing by 2° to 7°C by 2100 (Cayan et al. 2008). Assuming a similar distribution change in temperature in March and April, we can calculate a projection of the shift in SCD by the end of the century. Using the relationship between temperature and SCD anomalies in Fig. 6b, this implies a shift in the SCD from current mean values by 6 to 21 days earlier by the end of the century, with potentially much larger shifts in snowmelt runoff timing.

These extrapolations into the future may be too conservative because the trends in SCD found in this study are probably low estimates of future changes in peak snow mass timing. In addition to acceleration of climate change itself, snow season temperatures will begin to rise above the freezing point with increasing frequency as the climate continues to warm, leading to more precipitation falling as rain instead of snow. On average, this threshold has not yet been reached for the given stations during the months of March and April. During March and April there were only two instances (less than 0.1%) of data points shown in Fig. 5 having average daily minimum temperatures above 0°C. Most stations generally exhibit net snow accumulation during this time period. As minimum temperatures begin to rise above the critical threshold of 0°C much more often, melt rates will continue to increase, but precipitation will also shift from being dominated by snow to rain, which will eventually result in net melt rather than net accumulation in early spring. At present, January and February have both average daily maximum and minimum temperatures below freezing. If these winter months begin to experience temperatures above freezing, less accumulation may occur during this time, making the snowpack more susceptible to temperature fluctuations later in the season. Stations at lower elevations will be the first to exhibit changes in accumulation dynamics. This has been shown in Knowles et al. (2006), where sites at elevations below the majority of those in this study (below 1900 m) have exhibited a shift in cold season precipitation from snow to rain. The shift to rain will also impact SWE values in the latest part of the season first, which will contribute to the advance of SCD. The calculated sensitivity of SCD to late season temperatures does not reflect this mechanism yet, and therefore is probably a lower bound.

Given the importance of high-resolution snowpack predictions, continued research on the California Sierra Nevada snowpack is critical to understanding the state's future water supply. Continuation of SWE measurements is necessary to monitor and predict changes in the water supply from the Sierra Nevada snowpack. Regional modeling studies of the Sierra Nevada would also be helpful to determine the mechanisms affecting accumulation and melt events and to identify regions where precipitation will shift from being snow-dominated to rain-dominated. Snowmelt runoff will be affected by changes in snowfall amounts and snowmelt timing. An understanding of the mechanisms affecting these variables will help predict the future of the California water supply.

Acknowledgments. Sarah Kapnick is supported by an NASA Earth and Space Science Fellowship (#07-Earth07F-0232) and a JPL fellowship (Earth Climate Science: Collaborative Investigations with UCLA Graduate Students: 1313181). Alex Hall is supported by UC Water Resources Grant WR1024. The writers would also like to gratefully acknowledge funding provided by JPL (#1312546) under a project entitled: ''Evaluating key uncertainties in IPCC Climate Change projection of California snowpack: Topography, snow, physics and aerosol deposition.''

APPENDIX

Test of Snow Station Coherence

If stations exhibit different accumulation patterns—entirely possible given their broad geographical and altitudinal distribution—they must be treated as subgroups of data rather than as a single system to avoid overgeneralization of the behavior of the snowpack. Understanding the spatial variability of SWE is therefore a necessary step in our study. To achieve this, we calculate the spatial coherence of the monthly SWE values. The

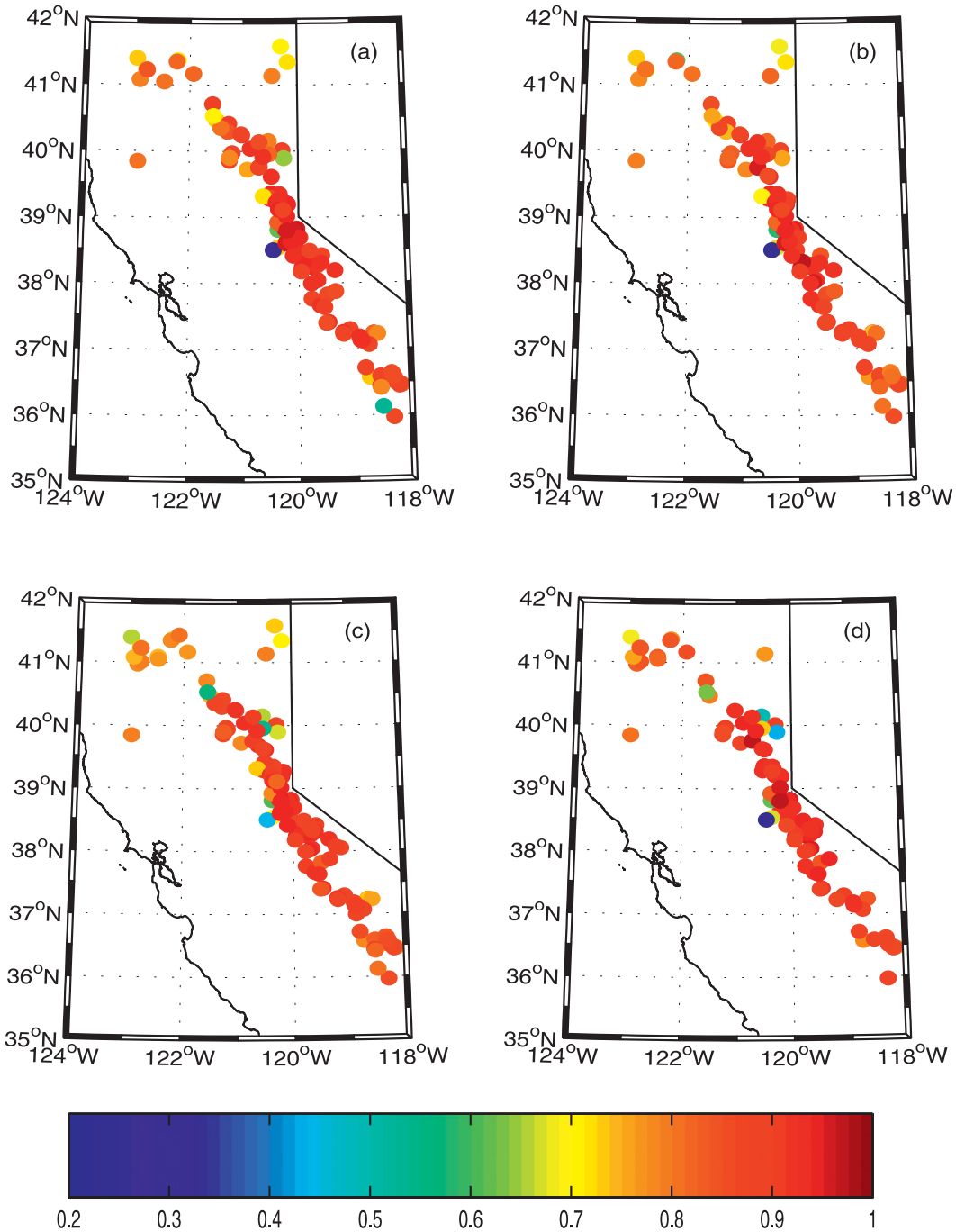

FIG. A1. Correlation plot to show spatial station coherence. Correlations are calculated on a first-of-the-month basis for (a) February, (b) March, (c) April, and (d) May. For the given month, correlations were calculated on a station-by-station basis between individual station SWE values against the mean SWE value for the set stations shown. Only stations with annual data for at least 50% of the record between 1930 and 2008 are used. There were 119, 120, 139, and 102 stations, respectively, in each month.

subset of stations for each month (taken within two weeks of the first of the month in February, March, April, and May) with yearly values available for 50% of the time period from 1930 to 2008 is used for this analysis. For each month, the time series of SWE values averaged over the state are calculated and then correlated with each individual station time series. The results are then plotted in Fig. A1.

We find that snow stations are generally highly spatially correlated with the mean SWE value for the snowpack, especially those stations below 40°N. For example, in the month of April, 110 stations have correlations to the mean SWE value above 0.80 with $p < 0.01$. This pattern persists from February to May, implying SWE anomalies are fairly uniform across the state for all months. These correlations may also be lower than if the analysis was conducted with actual first-of-the-month SWE values given that measurements are taken within two weeks of the first of the month. This measurement practice may introduce some error in these correlation calculations. However, the overall spatial coherence of snowpack variability demonstrates that minor temporal gaps at individual stations will not materially affect analysis of the climatology and variability of the overall California snowpack when the dataset is taken as a coherent group. This finding is especially important for the trend analysis found in section 3b and shown in Fig. 3 as some stations do not have data over the entire time period of interest (1930 to 2008). Sensitivity analysis of calculated trends is also provided when stations with different temporal records are used (Table 1).

It should be noted that the station below 40°N with the lowest correlation to the mean SWE time series is also the station with the lowest elevation. This location likely has different meteorological conditions, temperature patterns, and may experience snowmelt earlier and more frequently throughout the snow accumulation season than points at higher elevation. Because of its aberrant behavior, this station is left out of other analysis conducted in this study.

REFERENCES

Aguado, E., D. Cayan, L. Riddle, and M. Roos, 1992: Climatic fluctuations and the timing of west coast streamflow. *J. Climate,* **5,** 1468–1483.

Barnett, T., and Coauthors, 2008: Human-induced changes in the hydrology of the western United States. *Science,* **319,** 1080–1083, doi:10.1126/science.1152538.

Cayan, D., 1996: Interannual climate variability and snowpack in the western United States. *J. Climate,* **9,** 928–948.

——, S. Kammerdiener, M. Dettinger, J. Caprio, and D. Peterson, 2001: Changes in the onset of spring in the western United States. *Bull. Amer. Meteor. Soc.,* **82,** 339–415.

——, E. Maurer, M. Dettinger, M. Tyree, and K. Hayhoe, 2008: Climate change scenarios for the California region. *Climatic Change,* **87** (S1), 21–42.

Hamlet, A., and D. Lettenmaier, 2005: Production of temporally consistent gridded precipitation and temperature fields for the continental United States. *J. Hydrometeor.,* **6,** 330–336.

——, P. Mote, M. Clark, and D. Lettenmaier, 2005: Effects of temperature and precipitation variability on snowpack trends in the western United States. *J. Climate,* **18,** 4545–4560.

Huntington, T., G. Hodgkins, B. Keim, and R. Dudley, 2004: Changes in the proportion of precipitation occurring as snow in New England (1949–2000). *J. Climate,* **17,** 2626–2636.

Knowles, N., M. Dettinger, and D. Cayan, 2006: Trends in snowfall versus rainfall in the western United States. *J. Climate,* **19,** 4545–4559.

Lundquist, J., D. Cayan, and M. Dettinger, 2004: Spring onset in the Sierra Nevada: When is snowmelt independent of elevation? *J. Hydrometeor.,* **5,** 327–342.

Mote, P., 2006: Climate-driven variability and trends in mountain snowpack in western North America. *J. Climate,* **19,** 6209–6220.

——, A. Hamlet, M. Clark, and D. Lettenmaier, 2005: Declining mountain snowpack in western North America. *Bull. Amer. Meteor. Soc.,* **86,** 39–49.

Pierce, D., and Coauthors, 2008: Attribution of declining western U.S. snowpack to human effects. *J. Climate,* **21,** 6425–6444.

Regonda, S., B. Rajagopalan, M. Clark, and J. Pitlick, 2005: Seasonal cycle shifts in hydroclimatology over the western United States. *J. Climate,* **18,** 372–384.

Serreze, M., M. Clark, R. Armstrong, D. McGinnis, and R. Pulwarty, 1999: Characteristics of the western United States snowpack from snowpack telemetry (SNOTEL) data. *Water Resour. Res.,* **35,** 2145–2160.

Stewart, I., D. Cayan, and M. Dettinger, 2004: Changes in snowmelt runoff timing in western North America under a 'business as usual' climate change scenario. *Climatic Change,* **62,** 217–232.

——, ——, and ——, 2005: Changes toward earlier streamflow timing across western North America. *J. Climate,* **18,** 1136–1155.